



Cite this: *RSC Adv.*, 2022, **12**, 27781

Combining multiple acquisition modes and computational data annotation for structural characterization in traditional Chinese medicine: Miao Nationality medicine Qijiao Shengbai Capsule as a case study[†]

Chi Ma, ^a Yuhao Zhang, ^c Xiuxiu Dou, ^a Li Liu, ^d Weidong Zhang ^{*abc} and Ji Ye ^{*b}

Qijiao Shengbai Capsule (QSC) is a reputable Miao Nationality medicine used for treating leukopenia, but its chemical composition has not yet been elucidated. We herein present a strategy, by integrating multiple data acquisition, computational data annotation and processing methods to visualize and identify the complicated constituents in QSC based on ultra-high-performance liquid chromatography coupled with traveling wave ion mobility quadrupole time-of-flight mass spectrometry (UPLC-TWIMS-QTOF-MS). The multiple data acquisition modes, including data-independent mass spectrometry^{Energy} (MS^E), data-independent high-definition mass spectrometry^{Energy} (HDMS^E), and fast data-dependent acquisition (fast-DDA), in both positive and negative ion modes, were conducted on a Waters-SYNAAPT G2-Si mass spectrometer with an ESI source. An in-house library built by the UNIFI platform could efficiently process the peak annotation of known compounds, whilst different structural types were clustered in the molecular networks for the analogous classification and structural annotation of the unknown ones. Neutral loss, diagnostic ions, feature fragmentation behaviors, and community curation of mass spectrometry data of known compounds helped exploit those similar neighboring nodes of unknown compounds. Moreover, by combination of the predicted CCS values from CCS platform with the experimental CCS values from HDMS^E, as well as diagnostic fragment ions, isomer compounds were annotated. By integrating reference compound comparison, a total of 202 constituents, including 94 flavonoids, 12 saponins, 30 phthalides, 38 organic acids, 3 amino acids, 7 alkaloids and 18 others, were unambiguously characterized or tentatively identified in QSC. Among them, 5 potential new compounds were detected and 12 pairs of isomers were comprehensively distinguished. Conclusively, the established multiple acquisition modes, computational data processing and analysis strategy proved to be useful for the in-depth structural identification of QSC.

Received 28th July 2022

Accepted 21st September 2022

DOI: 10.1039/d2ra04720a

rsc.li/rsc-advances

Introduction

Due to the advantages of allopathic treatment and minimal toxic side effects, traditional Chinese medicine (TCM) has been used as an alternative therapy for the prevention and treatment of diseases. Tibetan, Uyghur, Mongolian, and Miao national minority medicines assembled by unique regional experiences

and distinctive cultural characteristics, have played prominent roles in TCM for the prevention and treatment of diseases for hundreds of years in China.^{1–4} Despite numerous clinical investigations demonstrating their efficacy, research into the active ingredients of ethnic medicines is still lacking, thus severely limiting the secondary development and application.

The development of analytical technologies has been recognized as an effective method to comprehensively investigate different polarities, contents, and molecular masses of plant metabolites in TCM. Currently, ultra-high-performance liquid chromatography coupled with quadrupole time-of-flight mass spectrometry (UPLC-QTOF-MS) is the most preferred choice for the characterization of the primary or secondary metabolites in complex matrices of herbal plants.^{5–7} Data-dependent acquisition (DDA)⁸ and data-independent acquisition (DIA)⁹ are the two most commonly used data acquisition modes for yielding the cleaner precursor-product links of the

^aInstitute of Interdisciplinary Integrative Medicine Research, Shanghai University of Traditional Chinese Medicine, Shanghai, 201203, China. E-mail: wdzhangy@hotmail.com; Tel: +86 021 81871244

^bSchool of Pharmacy, Naval Medical University, Shanghai 200433, China. E-mail: catheline620@163.com; Tel: +86 021 81871248

^cSchool of Traditional Chinese Pharmacy, China Pharmaceutical University, Nanjing, 211198, China

^dGuizhou Hanfang Pharmaceutical Co., Ltd., Guizhou, 550014, China

[†] Electronic supplementary information (ESI) available. See <https://doi.org/10.1039/d2ra04720a>



top N most intense MS peak and the higher coverage of all the MS/MS information of the observing components, respectively. The individual usage of the above acquisition modes has the limitation of ignoring some minor trace compounds or interpreting the co-eluting ions. Therefore, integrated DIA and DDA acquisition modes, which could produce complementary mass spectrometry information from each other, were applied for the comprehensive characterization of compounds from herbal medicines.¹⁰ Moreover, considering that natural herbal medicines often contained the identical structures of isomers with similar chromatographic retention behaviors that could hardly be separated or detected by common modes of the instrument, the ion mobility model was introduced as an additional dimension of ions separation based on their charge state, size and shape.¹¹

The exploitation of mass spectrometry data in different scan modes offers the opportunity to analyze chemical components from multiple perspectives. With the progress of computer-aided composition analysis techniques, mass spectrometry data annotation tools have been developed for showing the intuitive results of the data and replacing the laborious manual work. Taking the advantages of multiple data processing methods in UNIFI software, which includes Common Fragmentation Search (CFS), Extracted Ion Chromatogram (EIC), Mass Defect Filter (MDF) and Neutral Loss Scan (NLS),¹² known constituents could be rapidly assigned and identified by comparison their MS and MS/MS information with the self-built database.¹³ Global natural products social molecular networking (GNPS, <https://gnps.ucsd.edu>) can form a visual molecular network through fast-DDA mass spectrometry data processing, and the correlation of individual nodes becomes a prominent mean of inferring unknown compounds.¹⁴ In addition, ALLCCS was a commonly used platform for providing the theoretical value of potential collision cross sections (CCS) during structural characterization of the isomers.^{15,16} By integrating the above computational data annotation and process platforms with various acquisition modes, accuracy and efficiency for clarifying the chemical composition in the complex system would be dramatically increased.

Qijiao Shengbai Capsule (QSC) is a well-known Miao Nationality medicine in China that consists of seven Chinese medicines, including *Indigofera stachyoides* Lindl. (IS, Xue Renshen), *Astragalus membranaceus* (Fisch.) Bge. var. *mongholicus* (Bge.) Hsiao (AM, Huang Qi), *Equus asinum* L. (EA, E Jiao), *Angelica sinensis* (Oliv.) Diels (AS, Dang Gui), *Ziziphus jujuba* Mill. (ZJ, Da Zao), *Sophora flavescens* Ait. (SF, Ku Shen) and *Epimedium brevicornu* Maxim. (EB, Yin Yanghuo) with a ratio of 3 : 6 : 2 : 2 : 2 : 2 : 3. It has been patented for treating leukopenia in clinic and is capable of increasing vitality and ameliorating anemia.¹⁷ Modern pharmacological study showed that it has effectiveness on adjusting immune.^{18,19} To the best of our knowledge, no systematic chemical composition studies on QSC have been published.

The aim of our current work was to integrate multiple data acquisition modes of MS^E, fast-DDA and HDMS^E on a powerful traveling wave ion mobility TOF-MS coupled with UPLC and data processing of UNIFI, molecular networking, CCS platforms

for systematic profiling and annotating of known, unknown components and their co-eluting isomers from QSC. This is the first study on comprehensive chemical composition analysis of QSC, which will be beneficial for the further development of the guidelines for controlling its quality and the interpretation of its inherent pharmacology and mechanism of action on treating leukopenia.

Experimental

Materials

A total of 47 reference compounds were used in the qualitative identification of compounds in QSC. L-Hydroxyproline, protocatechuic acid, daidzein, emodin and ferulic acid were purchased from National Institutes for Food and Drug Control (Beijing, China). L-Proline, leucine, sophoridine, quinic acid and chlorogenic acid were purchased from Shanghai Ruiding Chemical Co., Ltd. (Shanghai, China). Ammonium, hyperoside, icariin, soyasaponin I and icaritin were purchased from Shanghai Liding Biotech Co., Ltd. (Shanghai, China). Gentisic acid, oleanic acid and *p*-hydroxycinnamate were purchased from Shanghai Adamas Biotech Co., Ltd. (Shanghai, China). Isoxanthohumol was purchased from Sigma Aldrich (Sigma, St. Louis, MO). Medicarpin and calycosin-7-O- β -D-glucoside were purchased from Shanghai Tauto Biotech Co., Ltd. (Shanghai, China). Matrine, epimedin A, epimedin B, epimedin C, astragaloside IV, astragaloside III and astragaloside I were purchased from Shanghai Chenguang Biotech Co., Ltd. (Shanghai, China). Magnoflorine, calycosin and betulinic acid were purchased from Shanghai Yuanye Biotechnology Co., Ltd. (Shanghai, China). Kaempferitrin, isoquercitrin, senkyunolide I, senkyunolide H, senkyunolide A, cycloastragenol and ligustilide were purchased from Sichuan Weikeqi Biotech Co., Ltd. (Sichuan, China). Formononetin and baohuoside I were purchased from Mansite Pharmaceutical Technology Co., Ltd. (Chengdu, China). Tokinolide B, riliguistilide, angelicide, levistolide A, maackiain, butylidene phthalide and butylphthalide were purchased from Desite Pharmaceutical Technology Co., Ltd. (Chengdu, China). All reference standards were determined with the purities of more than 95% by HPLC, and their structural information is presented in Fig. 1. QSC samples (lot number: 2520029) and its seven herbal medicines were generously provided by Guizhou Hanfang Pharmaceutical Co., Ltd. (Guiyang, China). LC-MS grade acetonitrile, formic acid, water and methanol were purchased from Fisher Scientific Co. (Fair Lawn, NJ, USA); leucine enkephalin was obtained from Sigma-Aldrich (St. Louis, MO, USA). All the other reagents were of analytical grade.

Samples and reference solutions preparation

Stock solutions of 47 reference compounds were dissolved in appropriate amount of methanol to produce the concentration of each of 1 mg mL⁻¹, and were stored at 4 °C until analysis. Then, we dilute them with 80% methanol to produce a mixture solution containing approximately 50 µg of each per mL as the reference solution before injection.



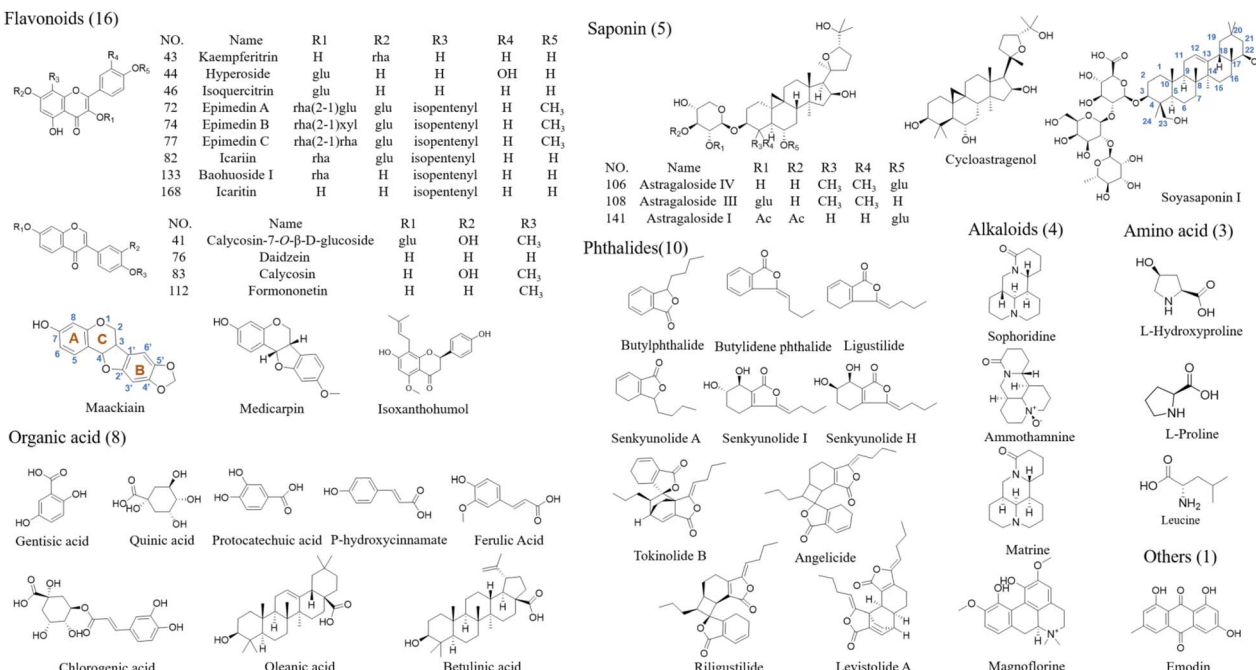
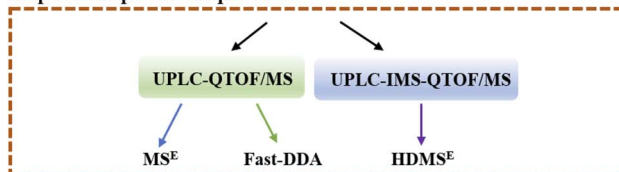


Fig. 1 Chemical structures of 47 reference substance.

Step 1. Sample preparation



Step 2. Multiple data acquisition



Step 3. Computational data annotation and processing

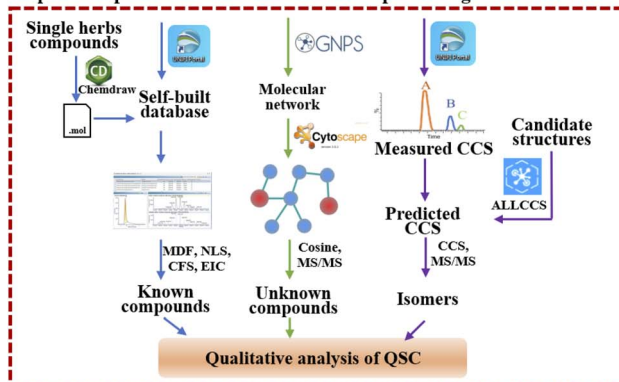


Fig. 2 A workflow for multiple data acquisition and computational annotation of the chemical composition of QSC.

The outer layer of QSC was removed, and the seven crude drug materials were separately pulverized to fine powders (pass through a 40-mesh sieve). 5.0 g of each of QSC and the above-mentioned powders were weighed accurately and then were ultrasonically extracted by 50 mL of 80% methanol (power 300 W, frequency 40 kHz) at room temperature for 45 minutes, respectively, yielding the test solutions of QSC and seven individual crude drugs. All the reference solutions and test solutions were centrifuged at 12 000 rpm for 10 min, and the supernatant was stored at 4 °C before analysis.

Liquid chromatographic analysis condition

The chromatographic analysis of QSC was obtained using an ACQUITY UPLC I-class system (Waters, Milford, MA, USA) equipped with a binary solvent delivery system, an autosampler, a degasser and a thermostat column compartment. The separation of samples was performed on a Waters ACQUITY HSS T3 C₁₈ reversed phase column (2.1 mm × 150 mm, 1.8 μm, Waters, Milford, MA, USA). The mobile phase was consisted of 0.1% formic acid in water (v/v, A) and acetonitrile (B) with gradient elution: 0–2.0 min, 8–8% B; 2.0–10.0 min, 8–30% B; 10.0–18.0 min, 30–50% B; 18.0–20.0 min, 50–65% B; 20.0–30.0 min, 65–100% B; 30.0–30.1 min, and then equilibrated at 8% for three minutes. The flow rate was kept at 0.25 mL min⁻¹. The column temperature and autosampler temperature were maintained at 35 °C and 4 °C, respectively. The injection volume was set as 2 μL.

Mass spectrometry conditions

Electrospray ionization (ESI) source parameters. The UPLC system was coupled with a Waters TWIM-QTOF-MS detector



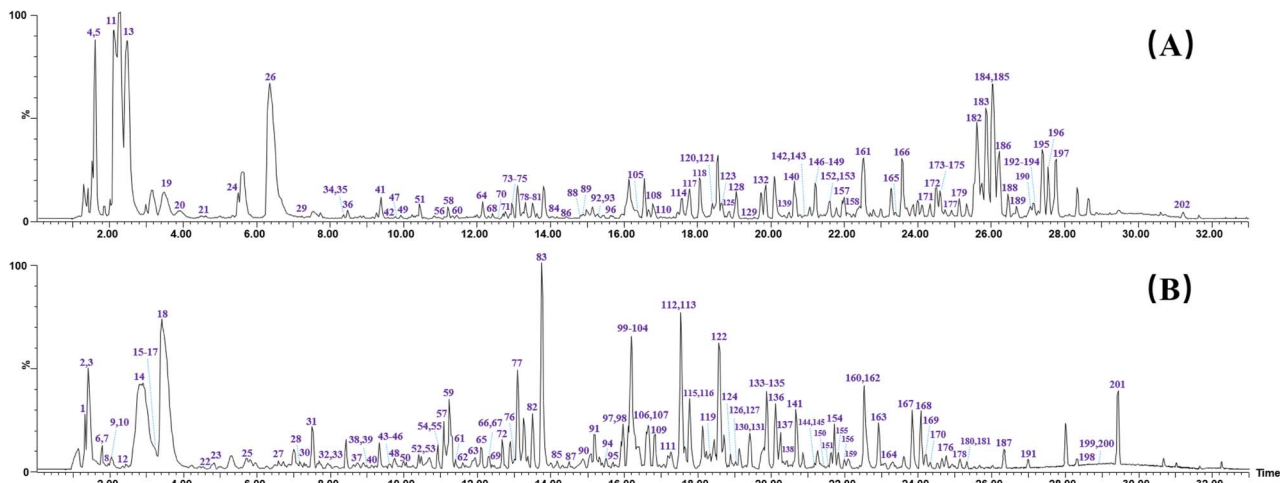


Fig. 3 The representative base peak chromatograms (BPCs) chromatogram of QSC by UPLC-QTOF-MS^E in positive (A) and negative (B) ion modes.

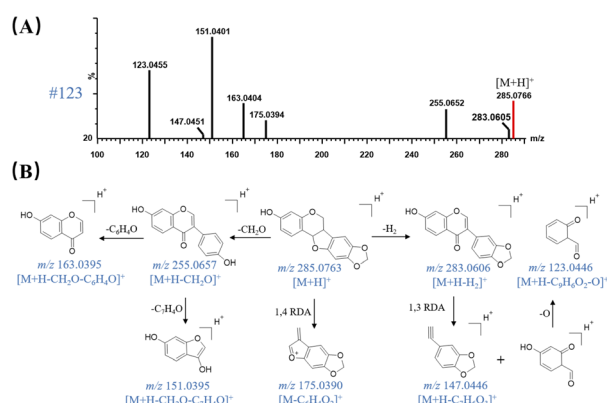


Fig. 4 MS^E spectra and proposed fragmentation pathway of maackiain in QSC under positive ion mode. (A) MS/MS spectra of #123 with parent ion at m/z 285.0766 $[M + H]^+$, (B) proposed fragmentation pathway of maackiain.

(Waters Corp., Manchester, UK) with an ESI source. The ESI parameters were optimized as follows: capillary voltage, 3.0 kV in positive ion mode and 2.5 kV in negative ion mode; sampling cone voltage, 40 V, source offset, 80 V; ion source temperature, 100 °C; desolvation temperature, 400 °C; cone gas flow, 50 L h⁻¹; desolvation gas flow rate, 800 L h⁻¹.

Data acquisition parameters. Mass spectral data of three dimensions were acquired to yield abundant MS fragmentation information. For data acquisition parameters under MS^E mode, the scan time was limited as 0.3 s. Two scan functions were carried out, with collision energy and collision energy ramp optimized at 6 eV and 10–45 eV in function 1 and function 2, respectively. The cone voltage which overrides cone voltage value specified in tune file was set at 40 V. For data acquisition parameters under HDMS^E mode, the flow rate of the MassLynx V4.1 software the buffer gas nitrogen (N₂) was 25 mL min⁻¹. The wave velocity was 650 m s⁻¹ and the pulse height tuned at 15 V. Polyalanine at a concentration of 10 mg mL⁻¹ in methanol was

used as a calibration reagent in CCS calibration. For data acquisition parameters under fast-DDA mode, the MS and MS/MS scan rate was 0.2 s. The maximum number of ions which can be selected for MS/MS from a single MS survey scan was limited as 5. The dynamic peak exclusion was turned on. The acquire and then exclude time was set at 6 s. The MS/MS collision energies was optimized at 6–40 V for low mass collision energy whilst 40–120 V was selected for high mass collision energy. All the mass spectra were acquired in both positive ion mode and negative ion mode. N₂ and argon (Ar) were applied as cone and collision gases, respectively. The mass range was set as m/z 50–1200 Da. The SYNAPT G2-Si system was calibrated using sodium formate solution and data was acquired in resolution mode. Leucine enkephalin at a concentration of 200 pg μ L⁻¹ was used as an external reference (Lock-SprayTM) to calibrate the real-time data, locking the mass at m/z 556.2771 in positive ion mode and m/z 554.2615 in negative ion mode.

Structural database construction of QSC

The database of QSC was built at UNIFI platform by searching literature and online databases of CNKI, PubMed, ChemSpider, PubChem, Sci-finder, Chemical Book, and Web of Science. As a result, a self-built database of which containing compound name, chemical structure, molecular formula and precise molecular weight information for a total of 927 chemical components in the seven Chinese medicines of QSC was initially constructed. The database was apt to provide adequate MS and MS/MS ions information for the further qualitative analysis.

UNIFI parameters for MS^E and HDMS^E

For analyzing the data under MS^E acquisition mode, the retention time (RT) range was set at 0.1–33.0 min, with the tolerance of \pm 0.2 min. The mass range was 50–1200 Da and the mass accuracy tolerance was set at \pm 5 ppm. The adducts of +H, +Na, -e and -H, +COOH were selected in positive ion mode



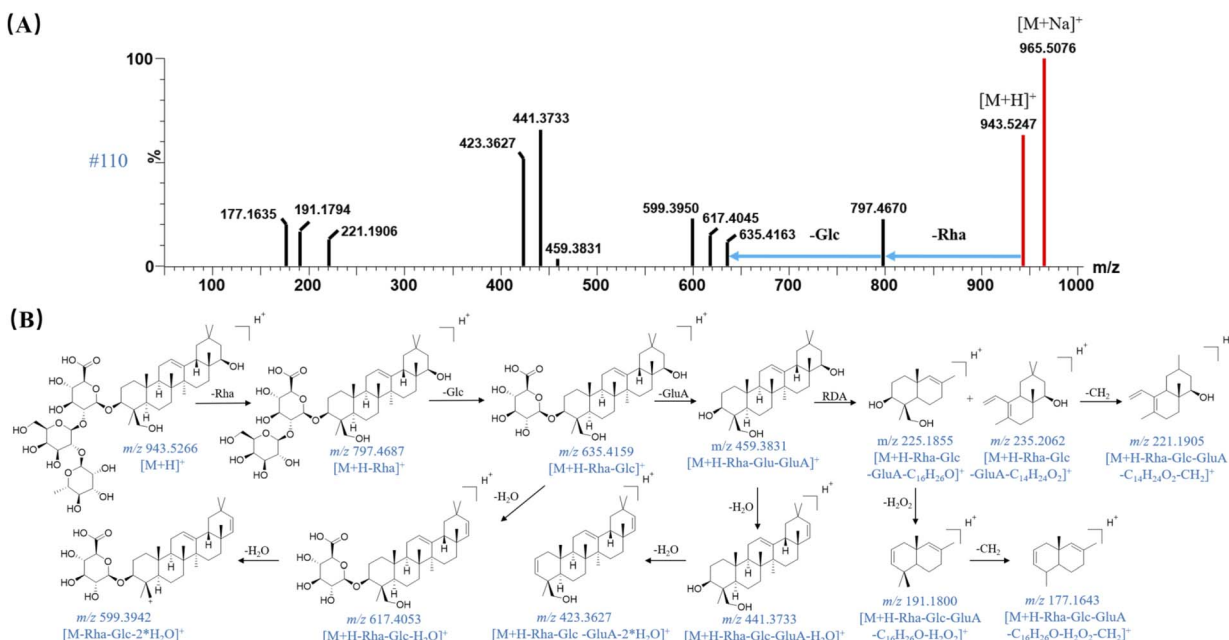


Fig. 5 MS^E spectra and proposed fragmentation pathway of soyasaponin I in QSC under positive ion mode. (A) MS/MS spectra of #110 with parent ion at m/z 965.5076 $[M + Na]^+$, (B) proposed fragmentation pathway of soyasaponin I.

and negative ion mode, respectively. The peak intensities of low energy over 1000 counts and high energy over 300 counts were optimized as parameters in 3-dimensional peak detection.

For analyzing the data under $HDMS^E$ acquisition mode, the RT started at 1.0 minutes and ended at 33.0 minutes. The mass range in high collision energy was started at 50 Da and ended at 800 Da, and in low collision energy was started at 50 Da and ended at 350 Da. The intensity threshold was optimized at 10 counts. The target match tolerance was tuned at 20 ppm. The fragment match tolerance was set at 30 ppm. The collision cross section tolerance was limited as 2.0%.

Molecular network parameters

In the GNPS platform, the precursor ion mass tolerance was set to 2.0 Da and a MS/MS fragment ion tolerance of 0.5 Da. The ion filtering window for all MS/MS fragments of precursor m/z was ± 17 Da, while the filtering window for MS/MS spectrum was ± 50 Da. The matched peaks and the cosine score were set to be more than 6.0 and 0.7, respectively. The maximum size of a molecular family was set to 100. The molecular network was generated and downloaded from the platform.

Collision cross sections condition

Experimental validation of collision cross-sections. Lock-Mass and LockCCS are performed to ensure the accuracy and precision of the instrument. The instrument was kept at 'Mobility TOF' condition for at least 1 hour, then CCS calibration was performed. Polyalanine was utilized as a calibration reagent. When the percent of RMS CCS (root mean square) is below 1%, the pre-calibration condition is satisfactory.

Prediction of collision cross-sections by web-enable platforms. ALLCCS (<https://allccs.zhulab.cn>) is an open-source CCS database for supporting the identification of unknown isomer compounds. The SMILES structures of those candidates, which were originated from $HDMS^E$ mode, were uploaded to these two platforms for yielding their corresponding predicted CCS values. ALLCCS contains a CCS database of more than 1.6 million compounds. All experimental CCS values are collected from published multiple datasets, independent labs, and instrument platforms. An average CCS value from instrument platforms is produced, showing a confidence level to restrict its error.²⁰ The platform allows efficient and rapid acquisition of theoretical CCS values for the isomers in the formula, which can be used as a preliminary prognosis for qualitative identification of isomers.

Experimental calculation of collision cross-sections. The $HDMS^E$ data of QSC was pre-processed by UNIFI platform and then the experimental CCS values were calculated by analyzing the four-dimensional data, including CCS, m/z , RT, and intensity. The CCS values are calculated according to the principles of the Mason-Schamp equation shown below.

$$\Omega = \frac{3}{16} \sqrt{\frac{2\pi}{\mu\kappa_B T}} \frac{ze}{NK}$$

where μ is the reduced mass of the ion and calculated by $(m_{\text{ion}} \times m_{\text{gas}})/(m_{\text{ion}} + m_{\text{gas}})$, m_{ion} and m_{gas} are the molecular masses of the analyte ion and drift gas, respectively. κ_B is the Boltzmann constant, T is the temperature, z is the electron charge, e is the unit charge capacity, N is the number density of particles and K is a constant related to an electron charge. The accurate CCS values of the candidate isomers were then calculated automatically by the equation.



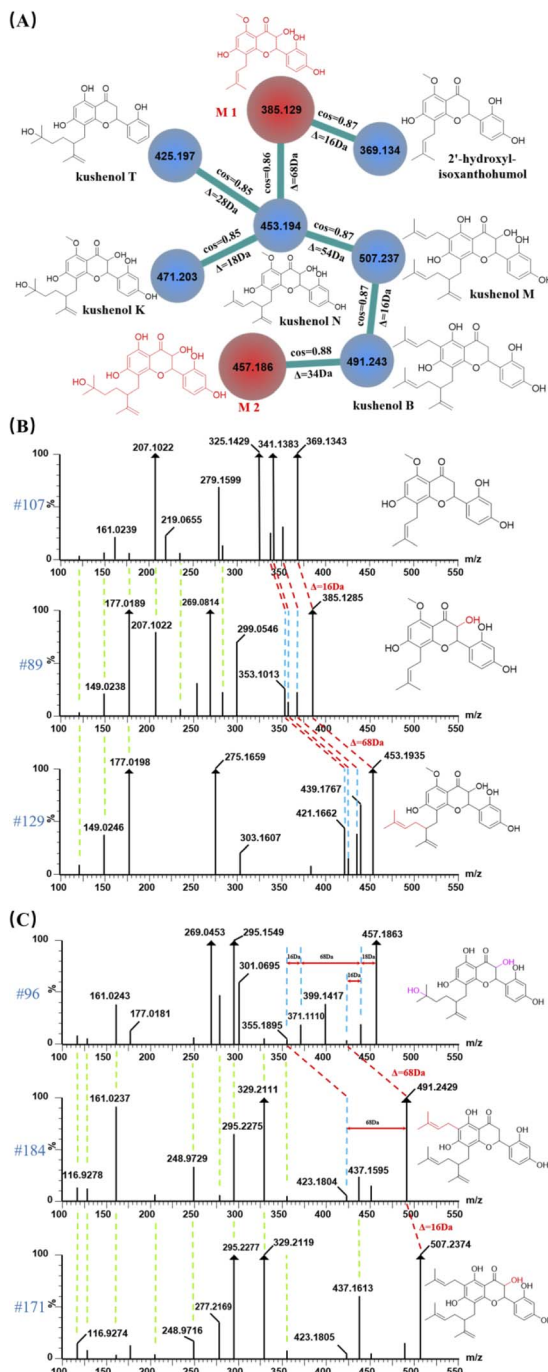


Fig. 6 The molecular network predicts the novel compounds in QSC. (A) The molecular network of isopentenyl flavonoids from SF. The blue nodes were the known compounds, while the red nodes were the unknown components. (B) MS/MS spectra and chemical structure of m/z 453 (peak 129), m/z 385 (peak 89) and m/z 369 (peak 107). (C) MS/MS spectra and chemical structure of m/z 507 (peak 171), m/z 491 (peak 184) and m/z 457 (peak 96). The groups marked with purple and red color were decreased and increased between two adjacent nodes, respectively. The green dashed line indicated that the fragment ions have the same m/z .

Data processing software

Mass spectrometry data acquisition was progressed in MassLynx V4.1 software. UNIFI™ version 1.8.0 (Waters, Manchester, UK) was applied to handle the processing and analysis

of MS^E and $HDMS^E$ mass spectrometry data to obtain match values for known compounds and CCS values of the target compounds, respectively. ALLCCS was employed to predict the CCS value of target compounds. Cytoscape 3.7.1 was utilized to analyze the molecular network downloaded from GNPS.

The integrative research strategy and compound characterization

In order to fully capture the mass spectrometry data for multi-component characterization, we use combined acquisition methods under MS^E , $HDMS^E$ and fast-DDA modes. Moreover, aiming to enhance the analysis efficiency and accuracy, the computational data annotation with UNIFI, GNPS and ALLCCS platforms were utilized (Fig. 2). The first step is to import the MS^E mass spectrometry data into the UNIFI platform and use the self-built in-house database to rapidly analyze the known chemical components of QSC. Next, fast-DDA mass spectrometry data was uploaded to the GNPS network platform and Cytoscape was used to analyze the correlation between adjacent nodes in the molecular network. The information of RT, m/z , and MS/MS for each node was used to predict unknown compounds. Finally, the qualitative identification of isomers was achieved by comparing the predicted CCS values of the target compounds on the ALLCCS platform with the measured CCS values obtained from $HDMS^E$ mass spectrometry data. The three-step analytical strategy allows for a thorough examination of known and novel compounds as well as isomers in QSC.

Results and discussion

According to the established strategy, chemical profiling of QSC were analyzed both in positive and negative ion modes by using UPLC-TWIMS-QTOF-MS. A total of 202 chemical components were detected, including 94 flavonoids, 12 saponins, 30 phthalides, 38 organic acids, 3 amino acids, 7 alkaloids and 18 other compounds. By comparison of RT, fragment ions and characteristic molecular ions with the reference substance, 47 compounds of them were unambiguously identified. The representative base peak chromatograms (BPCs) and mass spectral molecular networks are shown in Fig. 3 and S1.† Table S1† displays the detailed information of each compound in QSC, including compound name, RT, formula, source, adduct ion, observed m/z , mass error and fragment ions.

Multi-components annotation from QSC by analyzing MS^E in both positive and negative ionization modes

MS^E has an advantage of the high coverage of precursor ions, therefore, producing abundant precursor-to-fragment ions of each compound in the raw UPLC-QTOF-MS profiles of QSC. By automatically searching the m/z , RT and MS/MS spectrum data in self-built databases in UNIFI software, multiple mass spectrometry data were processed and the proposed known compounds were sorted by scoring through matching with the self-built in-house library. Efficient neutral loss (NL) and feature fragmentation diagnostic strategies were then applied to rapidly confirm the structures of the matched candidates. As a result,



Table 1 CCS prediction errors for six pairs of isomer reference substances

No.	Name	Formula	RT (min)	Adducts	<i>m/z</i>	Drift time (ms)	Measured CCS (Å ²)	ALLCCS (Å ²)	Relative error
1	Sophoridine	C ₁₅ H ₂₄ N ₂ O	1.59	+H	249.197	1.81	158.47	160.9051	-1.51%
	Matrine	C ₁₅ H ₂₄ N ₂ O	2.84	+H	249.201	1.78	157.75	160.7439	-1.86%
2	Senkyunolide I	C ₁₂ H ₁₆ O ₄	12.1	+Na	247.095	1.96	163.27	158.1086	3.26%
	Senkyunolide H	C ₁₂ H ₁₆ O ₄	12.65	+Na	247.096	1.95	162.96	158.1086	3.07%
3	Maackiain	C ₁₆ H ₁₂ O ₅	18.71	-H	283.062	2.26	166.14	170.2229	-2.40%
	Calycosin	C ₁₆ H ₁₂ O ₅	13.77	-H	283.061	2.19	164.09	166.4920	-1.44%
4	Butylphthalide	C ₁₂ H ₁₄ O ₂	22.01	+H	191.107	1.22	140.38	143.3732	-2.09%
	Ligustilide	C ₁₂ H ₁₄ O ₂	22.53	+H	191.106	1.28	142.85	143.5509	-0.49%
5	Tokinolide B	C ₂₄ H ₂₈ O ₄	25.85	+Na	403.188	3.61	203.87	195.9185	4.06%
	Riligustilide	C ₂₄ H ₂₈ O ₄	26.05	+Na	403.189	3.64	204.61	197.8284	3.43%
6	Angelicide	C ₂₄ H ₂₈ O ₄	26.05	+Na	403.189	3.63	204.35	197.8284	3.30%
	Levistolide A	C ₂₄ H ₂₈ O ₄	26.19	+Na	403.189	3.67	205.27	198.6753	3.32%
6	Betulinic acid	C ₃₀ H ₄₈ O ₃	28.54	-H	455.352	4.21	211.34	212.3275	-0.47%
	Oleanic acid	C ₃₀ H ₄₈ O ₃	29.01	-H	455.352	4.25	212.14	212.7024	-0.26%

a total of 155 compounds, including 87 flavonoids, 12 saponins, 26 organic acid, 10 phthalides, 3 amino acids, 7 alkaloids and 10 others were initially screened and 47 of them were tentatively confirmed by comparing their accurate mass measurements of MS, MS/MS and RTs with those of reference compounds.

Identification of flavonoids. In QSC, flavonoids are the major types of components in IS, EB, AM and SF. The basic skeleton structure of flavonoids is “C6–C3–C6”, with hydroxyl, methoxyl, isopentenyl, or glycosyl as substituent groups. In this study, a total of 92 flavonoids were detected and they were tentatively classified into flavones, isoflavones, flavonols, flavanones and isoflavanones due to their nucleus structures. Previous literature reported that retro-Diels–Alder (RDA) and C-ring fragmentation were the most possible fragmentation pathways for

flavonoids,^{21,22} yielding some typical fragment ions for the classification and structural identification of compounds. The positive ion mode MS^E data were primarily analyzed for the multicomponent characterization, while the negative data were interpreted as a supplementary.

Peak 123 (RT = 18.70 min) was taken as an example to elucidate the detection procedure and detailed fragmentation pathway of a derivative of isoflavanone. It showed a quasi-molecular [M + H]⁺ ion at *m/z* 285.0766 in MS scan mode. By matching with the in-house database in UNIFI platform, it was assumed as a known compound named maackiain, showing the molecular formula of C₁₆H₁₂O₅ with mass error of 1.05 ppm. Fig. 1 exhibits the chemical structure of maackiain and Fig. 4A presents its corresponding MS/MS spectra under proper

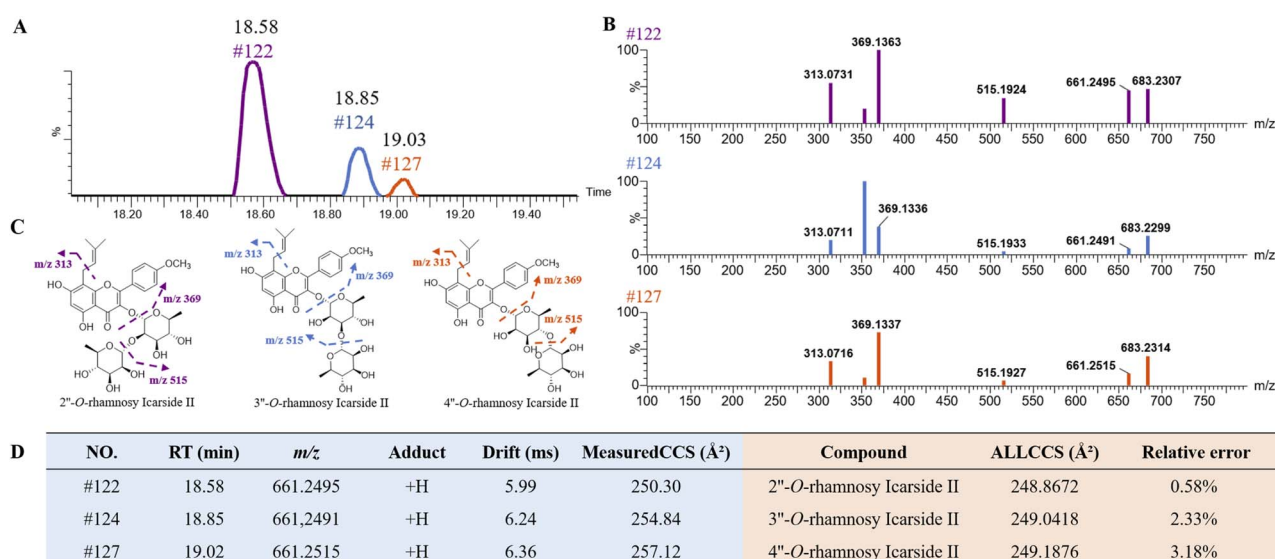


Fig. 7 Characterization of isomers with *m/z* 661.2496 and CCS prediction based on ALLCCS platform. (A) Three peaks in extracted ion chromatography (EIC) of *m/z* 661.2495 [M + H]⁺, (B) MS/MS spectra of three compounds (peak 122, 124 and 127), (C) fragmentation behaviors of 2"-O-rhamnosy Icarside II, 3"-O-rhamnosy Icarside II and 4"-O-rhamnosy Icarside II, (D) the RT, measured molecular weight, adducts, drift time, measured experimental CCS values and their predicted CCS values from ALLCCS platform of three compounds. Relative error represents the accuracy between measured experimental CCS values and predicted CCS values.



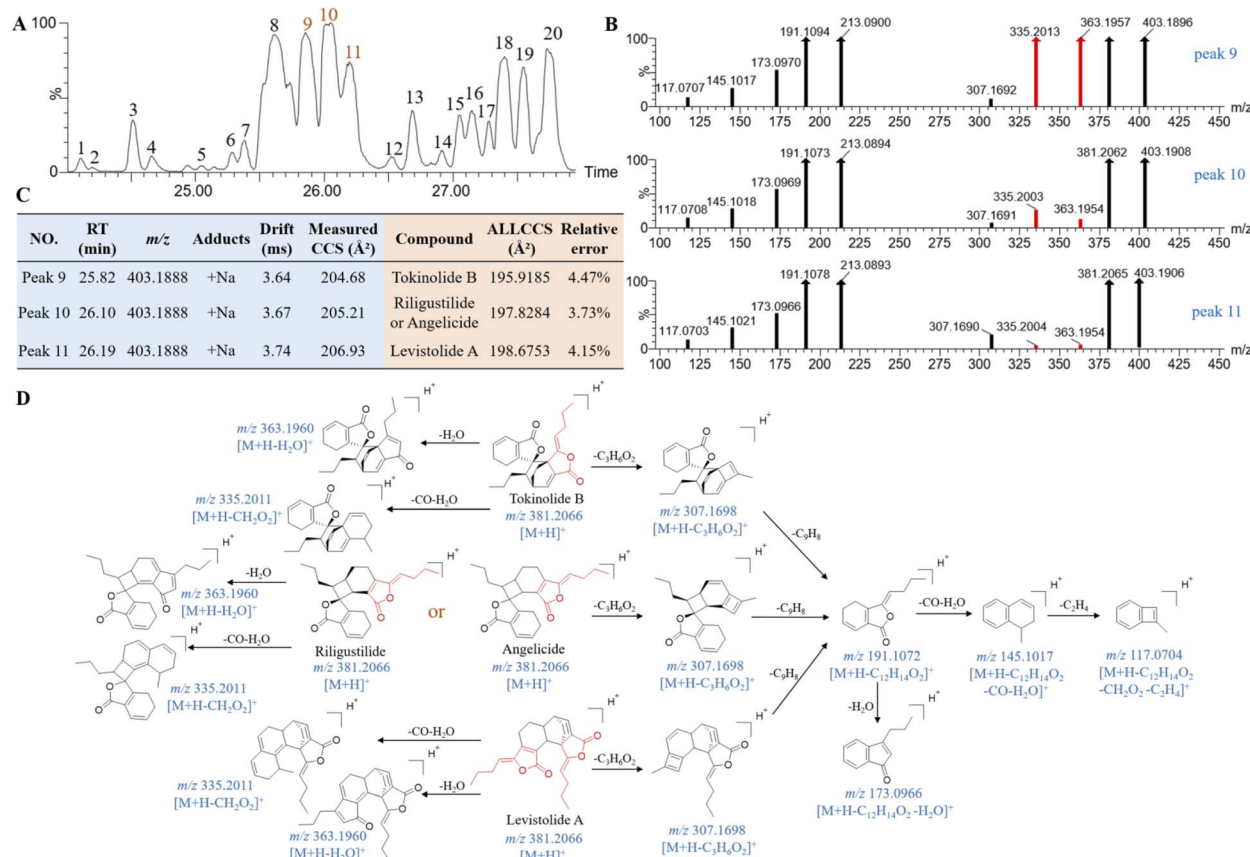


Fig. 8 Characterization of isomers with m/z 403.1885 and CCS prediction based on ALLCCS. (A) Twenty peaks in extracted ion chromatography (EIC) of m/z 403.1885 [$M + Na$]⁺, (B) MS/MS spectra of three peaks, (C) the RT, measured molecular weight, adducts, drift time, measured experimental CCS values and their predicted CCS values from ALLCCS platform of four reference compounds. Relative represents the accuracy between measured experimental CCS values and predicted CCS values, (D) fragmentation behaviors of tokinolide B, rilugustilide, angelicide and levistolide A.

collision energy. A serial of fragment ions at m/z 255, 175, 163, 151, 123, which were originated from the experiment, could be matched accurately with those proposed by computer with masse errors below 5 ppm. As shown in Fig. 4B, the B-ring side chain is apt to be opened, producing the $[M + H - CH_2O]^+$ ion at m/z 255. Then, the fragment ions at m/z 163 indicated the subsequent cleavage of the B-ring, which was consistent with the fragmentation behavior of flavonoid. When the substitution of hydroxyl on B ring, the cleavage of C ring is easy to be occurred.²¹ The m/z value obtained in the MS/MS for this ion is 151, which can be explained by opening the C-ring and the cleavage following by H atom transfer coming from C-2 position. On the other hand, after the loss of two H atoms from the precursor ion, the RDA cleavages at $^{1,3}A - ^{1,3}B$ -position were happened, giving rise to one fragment ions at m/z 147. Expel an oxygen atom (16 Da) was subsequently observed, leading to the production of daughter ion at m/z 123. We presumed it might be resulting from the fragment ion at m/z 139, another RDA product ions from m/z 283. The other pathways of maackiain also underwent the RDA cleavage at $^{1,4}A - ^{1,4}B$ -position, yielding the major product ions at m/z 175; this procedure was considered as a more stable chemical structure because it has a much

higher peak abundance. Based on the MS/MS spectra and retention behavior with standards compound and literature,²³ it was confirmed as maackiain and tentatively assigned to Miao Nationality herbal medicine named IS.

Isopentenyl type flavonoids were observed at high abundance in QSC, which were mainly originated from EB and SF. The presence of one or more isopentenyl groups (C_5H_8) is the most characteristic side chain of isopentenyl flavonoids. Due to the structural characteristics, the successively neutral loss of one or several isopentenyl group and its corresponding substituents were considered as the main fragmentation behaviors of this type components.²⁴ For example, peak 82 showed $[2M + Na]^+$ ion at m/z 1375.4617 in the full mass spectra scan, with RT of 13.52 min. It was identified by UNIFI platform as icariin with the elemental composition of $C_{33}H_{40}O_{15}$ and the mass error of -1.09 ppm. Its MS and MS/MS spectra showed two fragment ions at m/z 531 and 369 (Fig. S2A†), which were attributed to the neutral losses of rhamnose (Rha) and glucoside (Glc), respectively. It is worthy to note that the fragment ion at m/z 369 is apt to loss isopentenyl group of C_5H_8 (68 Da) and C_4H_7 (56 Da) at C-8 position, giving rise to the product ion at m/z 301 and 313, respectively. Then, the product ions at m/z 255 can



be explained by the loss of a CH_2O_2 (46 Da) from ion at m/z 301. The proposed fragmentation pathway of icariin was shown in Fig. S2B.† It was tentatively confirmed by comparing their accurate mass measurements of MS^E spectra and RTs with the reference compound. Thus, peak 82 was unambiguously identified as icariin.

Identification of saponins. Saponins were originated from AM in QSC. They had showed a wealth of precursor ions and product ions in positive ion mode. Neutral loss of Rha (146 Da), Glc (162 Da) and glucuronic acid (GluA, 176 Da) attributed to one or more glycoside bonds at the C-3 positions,²⁵ as well as the RDA cleavage at C-ring,^{25,26} were two key fragmentation pathways for those saponins in QSC. Peak 110 was induced as an example for elucidating the structural characterization and fragmentation behavior of saponins. Its MS/MS spectra and proposed fragmentation pathway were shown in Fig. 5. The precursor ion of it was m/z 965.5072 [$\text{M} + \text{Na}$]⁺ and the molecular formula was supposed to be $\text{C}_{48}\text{H}_{78}\text{O}_{18}$. Two various fragmentation patterns were summarized due to the skeleton of saponins. Due to one or several sugars attached to the hydroxyl group at C-3 position, neutral loss became one of the main cleavage pathways. Three typical fragment ions at m/z 797, 635 and 459 were in accordance with the successively neutral loss of Rha, Glc, and GluA. Subsequently, the ion at m/z 635 (hydroxyl group at the C-22 and C-23 position) underwent the loss of one or two molecular of H_2O , arising the dehydrated aglycone ions at m/z 617 and 599, respectively. Similarity, product ion at m/z 459 could experience the same fragmentation behavior, yielding two abundant fragment ions at m/z 441 and 423. RDA cleavages at C-ring was considered as the other main fragmentation patterns, owing to the presence of a double bond between C-12 and C-13. Due to the fragmentation behavior at C-ring, the key fragment ions of m/z 225 and 235 generated. Then, the ion at m/z 225 can easily undergo cleavage of the side chain, $-\text{OH}$ and $-\text{CH}_2\text{OH}$, with a relatively weak signal in MS/MS. It could produce the fragment ions at m/z 191, which were corresponded to the successive losses of $\text{H}_2\text{O} + \text{OH}$. In addition, the origin of ions at m/z 221 and 177 were presumed to be generated by losing of a methyl radical from ions at m/z 235 and 191. By comparison these fragmentation behaviors and the characteristic MS/MS information of standard, peak 110 was tentatively identified as a saponin named soyasaponin I. The result was consistent with that of UNIFI with the error of -1.04 ppm.

Identification of matrine-type alkaloids. Matrine-type alkaloids were the major constituents of SF, which show potential pharmacological activities on anti-tumor²⁷ and anti-COVID-19.²⁸ They exhibited high mass spectrometry responses in positive ion mode due to the additive of formic acid in the mobile phase. Generally, the matrine-type alkaloids are easy to experience the ring cleavage on the absence of unsaturated bonds of four rings. It contains two nitrogen atoms, one in the amide group and generally have no positive charge, whereas the other is basic and serves as the main location of the positive charge of the molecular ion. Thus, a large number of fragment ions were produced around this basic nitrogen, such as the characteristic fragment ions at m/z 148.²⁹ We use peak 19 as an example for illustrating its fragmentation pathways of matrine-type

alkaloids in QSC. The parent ion at m/z 249.1965 [$\text{M} + \text{H}$]⁺ (Fig. S3A†) was presumed as matrine in UNIFI platform, with the molecular formula of $\text{C}_{15}\text{H}_{24}\text{N}_2\text{O}$. MS/MS spectra showed fragment ions at m/z 247, 245, 176 and 150, arising from the elimination of 2 Da (H_2), 2 Da (H_2), 69 Da ($-\text{NH}-\text{CO}-\text{CH}-\text{CH}-$) and 95 Da ($-\text{CH}_2-\text{N}-\text{CO}-\text{CH}-\text{CH}-\text{CH}-$), respectively. The characteristic fragment ion at m/z 148 formed by further loss of 2 Da (H_2) of fragment ion at m/z 150, which was then followed by the loss of 14 Da (CH_2) with creating the fragment ions of m/z 136. The observation of the moderately intense ion at m/z 112 was attributed to loss of C_5H_4 from ion at m/z 176. The fragment ions at m/z 96 exhibited a strong MS/MS response and was obtained by the subsequent cleavage of 16 Da (CH_4) from ion at m/z 112. By integrating the information on MS/MS and the fragmentation pathways with those of reference compound, peak 19 was presumed to be matrine (Fig. S3B†).

Structural characterization of unknown compounds by molecular networks

After searching the in-house library or public databases, some of the untargeted compounds have not been annotated as the known compounds, and they were assumed to be presumed as unknown components. GNPS, an open-access knowledge platform, was able to process fast-DDA mass spectrometry data with creating a molecular network, in which the similarity of adjacent nodes has proven to be an effective tool for predicting new compounds.^{14,16} The GNPS platform has the advantage of integrating mass spectrometry data and visualizing the results, which has greatly facilitated the discovery of new compounds and reduced research time. GNPS first simplifies and merges the fast-DDA mass spectrum data and then reduces the pre-processed mass spectrum to vectors in a multi-dimensional normalized space where each dimension is assigned an m/z value and its respective intensity.³⁰ What's more, the results of these vector-based comparisons on GNPS can be visualized as a molecular network³¹ in which compounds with similar structures are tend to cluster together for facilitating analysis.

Those vectors are used to calculate the cosine score between each pair of potentially consistent mass spectra, allowing the determination of the degree of spectral similarity between them. The cosine score ranged from 0 to 1, and the closer the cosine is to 1, the more similar the spectrum is.³² Finally, different fragment ions and RTs between adjacent nodes were used to identify chemical structures. As a result, 13 compounds in QSC, including 4 flavonoids, 8 organic acids, and 1 other, were screened out and tentatively identified by neutral losses, diagnostic fragment ions, feature fragmentation behaviors, and community curation of mass spectrometry data of known compounds. Three of them were reported for the first time.

Compounds in the same structural type were apt to undergoing similar fragmentation behaviors. Due to the comparable mass spectral information and characteristic fragment ions, those compounds can easily aggregate in molecular networks to form a cluster on GNPS platform. Using known compounds as a starting point, clusters of different type compounds were effectively discovered and unknown compounds with highly



similar structure in each cluster were preliminarily identified. Peak 89 and peak 96 (the red nodes), who can hardly be identified by searching with in-house database in UNIFI platform, were taken as examples for clarifying their structures. Luckily, they were gathered in a same cluster in molecular network (Fig. 6A), implying the high similarity of their molecular structural. The adjacent nodes of m/z 385 were assigned as two known compounds (the blue nodes) with the base peak at m/z 453 (peak 129) and m/z 369 (peak 107), which have been identified as kushenol N³³ and 2'-hydroxy-isoxanthohumol³⁴ by searching with the in-house databases in UNIFI platform (Table S1†). Furthermore, the cosine scores of those adjacent nodes were 0.86 and 0.87, indicating the high consistent of molecular structure. The molecular weight difference between them is 68.0650 Da and 15.9942 Da, which were presumed as the structural of the isopentenyl group and hydroxyl group, respectively. Moreover, the difference of masses (68 Da and 16 Da) were also existed between multiple pairs of fragment ions, as well as the same low molecular weight fragment ions in the three compounds (Fig. 6B), indicating that they might be the same structural type compound with the similar fragmentation behavior. According to the previously published literature,³⁵ the C-3 position is more apt to having the linkage of hydroxyl group rather than other positions. Thus, the chemical structure of peak 89 with quasi-molecular ion at m/z 385 can be preliminarily identified as M1 (3,2'-di-hydroxyl-isoxanthohumol, as shown in Fig. 6A), with the molecular formula of $C_{21}H_{22}O_7$ [$M - H$]⁻ and the mass error of -0.52 ppm.

Node at m/z 457 (peak 96) was adjacent to node at m/z 491 (peak 184), which was identified as kushenol B in UNIFI platform, with the molecular formula of $C_{30}H_{36}O_6$ [$M - H$]⁻ and the mass error of -1.02 ppm. A series of fragment ions at m/z 116, 128, 161, 248, 279, 295, 329, 355 (Fig. 6C) were both found in peak 96 and 184, implying those two compounds share the same skeleton and have high similarity in their structures. Fragment ion at m/z 423.1804 was produced due to the neutral loss of isopentenyl group with mass of 68.0626 Da for peak 184, which was in agreement with fragmentation behavior in peak 96. However, the difference in molecular weight between them was 34.0566 Da instead of 68.0626 Da, indicating the presence of some other substituent groups. By searching the MS/MS of peak 96, a relatively weak fragment ion at m/z 439.1748 was found, which was 18 Da less than m/z 457 and was corresponded to the subsequent neutral losses of H_2O . Furthermore, the m/z 423 ion was produced by expelling an oxygen atom from the fragment ion of m/z 439, presuming the existent of another hydroxyl group. According to the literature,³⁵ the double bond in the isopentenyl group at C-2' position was apt to undergo an addition reaction with H_2O to form a hydroxyl group resulting in an increase in molecular weight of 18 Da. It is worth noting that isopentenyl groups are more apt to be expelling at C-6 position than other positions C-2' position. Using the above evidences together with the information of molecular network, peak 96 could unambiguously be identified as M2 (as shown in Fig. 6A), with the chemical formula of $C_{25}H_{30}O_8$ [$[M - H]^-$] and a mass error of 0.22 ppm.

The annotation of isomer with HDMS^E

Isomers are widely existed in the complex components of natural herbal medicines. The co-eluted constituents resulting from the isomers with the high similarity in their parent ions and fragment ions made the structural identification difficult, which is a bottleneck for large-scale untargeted analysis of drugs. TWIMS is a high throughput analytical method based on a separation mechanism in which gaseous ions, depending on their size, shape and charge, arrive at the mass spectrometer detector at different times (drift time) for the separation of isomers.³⁶ CCS value is a unique physical property of the ion that is independent of the matrix composition and highly repeatable across different measurements and instruments, which is reliable can be calculated by the Mason–Schamp equation for isomers identification in complex system. Recently, an increasing number of web-enable databases^{15,16} have been developed to annotate CCS value, which supplied as a supplementary for identifying the isomers from diagnostic fragment ions. Isomer compounds were annotated by comparing the measured CCS values of the target peak from the processed HDMS^E mass spectrometry data with the predicted values from ALLCCS database. The results indicated that those open-source databases can generate highly accurate CCS values for targeted compounds, which is a key part of achieving qualitative analysis. Ultimately, 45 compounds assigned to 12 species of isomers were tentatively identified. By comparison the experimental CCS values with predicted values from ALLCCS platform, six pairs of isomer reference compounds showed acceptable CCS prediction errors within 5.0 percent (Table 1). Moreover, the predicted values of isomers were similar in sequence with the CCS values results of the instrument.

Isopentenyl flavonoid glycosides are representative chemical constituents of EB. The high similarity in their MS/MS ion made them hardly be distinguished by neutral loss strategy. As shown in Fig. 7A, three peaks at RT of 18.58 min (peak 122), 18.85 min (peak 124) and 19.03 min (peak 127) were screened by extracting ion chromatography with the same quasi-molecular ion at m/z 661.2496 [$M + H$]⁺ ($C_{33}H_{40}O_{14}$). A series of fragment ions at m/z 515, 369 and 313 (Fig. 7B) were detected in those isomers, suggesting the successive losses of Rha, Rha and C_4H_7 (Fig. 7C), respectively. By comparison these fragmentation behaviors and the accurate mass of MS and MS/MS spectrum with previous literature report,³⁵ those three compounds were tentatively identified as 2''-O-rhamnosy icarside II or its isomer. According to the previous report,³⁵ the glycoside of flavonoids in EB are all bonded at the C-3 and C-7 positions, and the rhamnoside is only directly linked at C-3 position. The isomers of 2''-O-rhamnosy icarside II were presumed to be 3''-O-rhamnosy icarside II and 4'-O-rhamnosy icarside II. After uploading the structures on ALLCCS platform, the predicted CCS values were obtained and showed in Fig. 7D. The experimental CCS values were subsequently measured by the drift time of UPLC-TWIMS-QTOF-MS, which were highly consistent with the predicted values from both of ALLCCS platform, with prediction errors less than 3.18%. The results initially confirmed the accuracy of the



structural predictions of those isomers. Based on measured results, the CCS values of these three compounds were ranked as follows: peak 122 < peak 124 < peak 127. Additionally, the predicted CCS values of 2"-O-rhamnosy icarside II, 3"-O-rhamnosy icarside II and 4"-O-rhamnosy icarside II from ALLCCS were ranked as follows: 2"-O-rhamnosy icarside II < 3"-O-rhamnosy icarside II < 4"-O-rhamnosy icarside II. As a result, peak 122, 124 and 127 was identified as 2"-O-rhamnosy icarside II, 3"-O-rhamnosy icarside II and 4"-O-rhamnosy icarside II, respectively. This method has also been applied for identifying the isomers with parent ions at m/z 317.2093, including peak 175, 176, 177 and 179 (as shown in Fig. S4†). By comparing the order of predicted and experimental CCS values, those isomers were preliminary identification as 13-oxo-9E,11E-octadecatrienoic acid, 9-oxo-10E,12E-octadecatrienoic acid, 9(10)-epoxy-12Z,15Z-octadecadienoic acid and 13-hydroxy-6Z,9Z,11E-octadecatrienoic acid, respectively.

Some conformational difference isomers exhibit the high similarity in their MS/MS spectrum as the co-eluting peaks, which often bring great challenges for their structural characterization. A total of 20 isomers (Fig. 8A), with quasimolecular ion at m/z 403.1885, have been detected in QSC. They were originated from AS, and have showed the common fragment ions at m/z 191, 173, 145 and 117 (Fig. 8B and D), which were in accordance with those of ligustilide,³⁷ a phthalide component derived from AS. These isomers were presumed as the dimers of ligustilide, including tokinolide B, riligustilide, angelicide and levistolide A according to the literature.³⁸ By comparison the RT and the CCS value with the standards (Fig. 8C), peaks 9 and 11 were tentatively identified as tokinolide B and levistolide A, respectively. However, due to only conformational differences, riligustilide and angelicide were co-eluted at the same RT. Additionally, the predicted CCS values of them on ALLCCS platform were both 197.8284 Å², whilst the experimental values (Table 1) of the reference were also close (204.61 Å² and 204.35 Å²) and the response intensity of MS/MS fragment ions (Fig. S5A†) have no difference. Thus, they could be hardly identified by the difference of CCS value and the diagnostic fragment ions. It is the different site of dimer binding that lead to differences in the space resistance of the side chains and five-membered ring, resulting in the corresponding characteristic fragments response intensities. The characteristic fragment ions at m/z 363 and m/z 335 were produced by side chain and five-membered ring cleavage with the loss of H₂O and CO + H₂O from the parent ions (Fig. 8D). Meanwhile, the peak intensities of the two fragment ions were different in those isomers, which could be helpful for distinguishing them. These two typical fragment ions at m/z 363 and m/z 335 have been showed in high response in HDMS^E spectra of tokinolide B, moderate response in riligustilide and angelicide, and a comparative weak response in levistolide A. Thus, peak 8 could be preliminary identification as an isomer of tokinolide B, which has high response of ions at m/z 363 and m/z 335 (Fig. S5B†). Following this regularity, peaks 1–6 and peaks 7–8 as well as peaks 12–20 are tentatively identified as isomers of riligustilide or angelicide, tokinolide B and levistolide A, respectively.

Conclusions

In this study, a new integrated multiple data acquisition and processing strategy based on UPLC-TWIMS-QTOF-MS for accelerating the compounds identification of Miao Nationality medicine QSC capsule has been developed. A total of 202 compounds were tentatively identified, and 155 of them were tentatively screened by the in-house database of UNIFI platform whilst 47 of them were tentatively confirmed by comparing their accurate mass measurements of MS^E spectra and RTs with those of reference compounds. According to the cosine values and characteristic ions of the adjacent nodes in the molecular network, 13 constituents were identified from the analysis pattern in GNPS platform. Moreover, 12 pairs of isomers were further identified by comparison of their CCS values in the ALLCCS platform with those experimental CCS values as determined by TWIMS mass spectrometry, and their diagnostic fragment ions could efficiently distinguish the isomers. This study shows that the integrated strategy for multiple data acquisition of mass spectrometry data is appropriate for the identification and discovery of known and unknown compounds as well as isomers in QSC. It is worth noting that this work is a practical example of comprehensive qualitative and systematic analysis from complex matrices that could guide many other similar projects.

QSC has demonstrated a great therapeutic effect on leukocyte elevation in clinical practice, and the identified components tentatively played an important role in the therapeutic process. Further investigation is warranted for exploring the key metabolites of QSC and the function of the prototype components and metabolites in the treatment of elevated leukocytes. This research is valuable for serving as a basis for its further examination in the field of pharmacology and mechanism of action.

Conflicts of interest

There are no conflicts to declare.

Acknowledgements

This work was funded by National Natural Science Foundation of China (No. 82141203, 81772798), Shanghai Municipal Science and Technology Major Project (ZD2021CY001), Three-year Action Plan for Shanghai TCM Development and Inheritance Program [ZY(2021-2023)-0401], Innovation Team and Talents Cultivation Program of National Administration of Traditional Chinese Medicine (ZYYCXTDD-202004), Shanghai Engineering Research Center for the Preparation of Bioactive Natural Products (16DZ2280200).

References

- 1 M. K. Tang, L. L. Luo, C. Zhang, J. H. Wu and X. Y. Wang, *J. Tradit. Chin. Med. Sci.*, 2021, **8**, S22–S26.
- 2 Z. Y. Li, Y. Tu, H. T. Li, J. He, S. Que, G. P. Dong, M. S. Zhang, J. Q. Liu, X. L. Huang, X. R. Wang, M. Bolat, X. Feng,



F. B. Zhang and F. Jiang, *Zhongguo Zhongyao Zazhi*, 2020, **45**, 2265–2274.

3 Y. L. Wu, L. Zhao, L. F. Gu, A. Tilyek, B. Y. Yu and C. Z. Chai, *J. Ethnopharmacol.*, 2022, **283**, 114696.

4 T. Wuniqiemu, J. J. Qin, F. Z. Teng, M. Nabijan, J. Cui, L. Yi, W. F. Tang, X. Y. Zhu, M. Abduwaki, M. Nurahmat, Y. Wei and J. C. Dong, *J. Ethnopharmacol.*, 2021, **266**, 113343.

5 W. Zhang, M. W. Saif, G. E. Dutschman, X. Li, W. Lam, S. Bussom, Z. L. Jiang, M. Ye, E. Chu and Y. C. Cheng, *J. Chromatogr. A*, 2010, **1217**, 5785–5793.

6 S. F. Wang, P. H. Chen, W. Jiang, L. H. Wu, L. L. Chen, X. H. Fan, Y. Wang and Y. Y. Cheng, *J. Chromatogr. A*, 2014, **1348**, 105–124.

7 W. Z. Yang, X. Qiao, K. Li, J. R. Fan, T. Bo, D. A. Guo and M. Ye, *Acta Pharm. Sin. B*, 2016, **6**, 568–575.

8 V. Davies, J. Wandy, S. Weidt, J. J. Hooft, A. Miller, R. Daly and S. Rogers, *Anal. Chem.*, 2021, **93**, 5676–5683.

9 C. Gotti, F. Roux-Dalvai, C. Joly-Beauparlant, L. Mangnier, M. Leclercq and A. Droit, *J. Proteome Res.*, 2021, **20**, 4801–4814.

10 H. Li, M. Uittenbogaard, R. Navarro, M. Ahmed, A. Gropman, A. Chiaramello and L. Hao, *Mol. Omics*, 2022, **18**, 196–205.

11 A. Bianco, I. Neefjes, D. Alfaouri, H. Vehkamaki, T. Kurten, L. Ahonen, M. Passananti and J. Kangasluoma, *Talanta*, 2022, **243**, 123339.

12 M. Y. Liu, S. H. Zhao, Z. Q. Wang, Y. F. Wang, T. Liu, S. Li, C. C. Wang, H. T. Wang and P. F. Tu, *J. Chromatogr. B: Anal. Technol. Biomed. Life Sci.*, 2014, **949–950**, 115–126.

13 C. X. Zhang, T. T. Zuo, X. Y. Wang, H. D. Wang, Y. Hu, Z. Li, W. W. Li, L. Jia, Y. X. Qian, W. Z. Yang and H. S. Yu, *Molecules*, 2019, **24**, 2708.

14 T. F. Cheng, Y. H. Zhang, J. Ye, H. Z. Jin and W. D. Zhang, *J. Pharm. Biomed. Anal.*, 2020, **184**, 113197.

15 H. Zhu, X. Wu, J. Huo, J. Hou, H. Long, Z. Zhang, B. Wang, M. Tian, K. Chen, D. Guo, M. Lei and W. Wu, *J. Chromatogr. A*, 2021, **1653**, 462405.

16 Y. H. Zhang, H. B. Lei, J. F. Tao, W. L. Yuan, W. D. Zhang and J. Ye, *RSC Adv.*, 2021, **11**, 15546–15556.

17 X. P. Zhang, H. J. Yang, D. H. Zou, X. M. He, X. F. Yu and Y. F. Li, *Afr. J. Tradit., Complementary Altern. Med.*, 2016, **14**, 155–164.

18 H. Yan, X. Zhang and J. Li, *Journal of Hubei University of Chinese Medicine*, 2020, **22**, 70–73.

19 H. Xu, Y. P. Zheng and L. Duan, *Chin. J. Ethnomed. Ethnopharmacology*, 2021, **30**, 8–15.

20 Z. W. Zhou, M. D. Luo, X. Chen, Y. D. Yin, X. Xiong, R. H. Wang and Z. J. Zhu, *Nat. Commun.*, 2020, **11**, 4334.

21 W. Wu, C. Y. Yan, L. Li, Z. Q. Liu and S. Y. Liu, *J. Chromatogr. A*, 2004, **1047**, 213–220.

22 L. W. Qi, C. Y. Chen and P. Li, *Rapid Commun. Mass Spectrom.*, 2009, **23**, 3227–3242.

23 N. Gampe, A. Darczi, S. Lohner, S. Beni and L. Kursinszki, *J. Pharm. Biomed. Anal.*, 2016, **123**, 74–81.

24 X. P. Ding, X. T. Wang, L. L. Chen, Q. Guo, H. Wang, J. Qi and B. Y. Yu, *J. Chromatogr. A*, 2011, **1218**, 1227–1235.

25 Y. G. Mi, W. D. Hu, W. W. Li, S. Y. Wan, X. Y. Xu, M. Y. Liu, H. D. Wang, Q. X. Mei, Q. C. Chen, Y. Yang, B. X. Chen, M. T. Jiang, X. Li, W. Z. Yang and D. A. Guo, *Molecules*, 2022, **27**, 3647.

26 X. P. Qi, X. Y. Wang, T. F. Cheng, Q. L. Wu, N. Mi, X. M. Mu, X. Guo, G. Zhao, Z. J. Huang, J. Ye and W. D. Zhang, *J. Sep. Sci.*, 2019, **42**, 2748–2761.

27 Z. Lin, C. F. Huang, X. S. Liu and J. K. Jiang, *Basic Clin. Pharmacol. Toxicol.*, 2011, **108**, 304–309.

28 D. D. Hu, X. Chen, D. X. Li, H. L. Zhang, Y. W. Duan and Y. Huang, *Pharmaceutics*, 2022, **14**, 603.

29 T. T. Jong, M. R. Lee, Y. C. Chiang and S. T. Chiang, *J. Pharm. Biomed. Anal.*, 2006, **40**, 472–477.

30 A. M. Frank, N. Bandeira, Z. X. Shen, S. Tanner, S. P. Briggs, R. D. Smith and P. A. Pevzner, *J. Proteome Res.*, 2008, **7**, 113–122.

31 J. Watrous, P. Roach, T. Alexandrov, B. S. Heath, J. Y. Yang, R. D. Kersten, M. Voort, K. Pogliano, H. Gross, J. M. Raaijmakers, B. S. Moore, J. L. Laskin, N. Bandeira and P. C. Dorrestein, *Proc. Natl. Acad. Sci. U. S. A.*, 2012, **109**, 1743–1752.

32 A. M. Frank, M. E. Monroe, A. R. Shah, J. J. Carver, N. Bandeira, R. J. Moore, G. A. Anderson, R. D. Smith and P. A. Pevzner, *Nat. Methods*, 2011, **8**, 587–591.

33 Q. H. Zhang, J. B. Yu, Y. Y. Wang and W. K. Su, *Molecules*, 2016, **21**, 989.

34 X. Dong, X. N. Li, N. Li, H. M. Zhao, A. GuLa, X. Zhang, P. Zhang and B. Q. Bao, *J. Sep. Sci.*, 2019, **42**, 3382–3389.

35 W. H. Qin, Y. Yang, Q. Li and X. Liu, *Nat. Prod. Res. Dev.*, 2021, **33**, 1478–1490.

36 F. Lanucara, S. W. Holman, C. J. Gray and C. E. Evers, *Nat. Chem.*, 2014, **6**, 281–294.

37 L. L. Chen, J. Qi, Y. X. Chang, D. N. Zhu and B. Y. Yu, *J. Pharm. Biomed. Anal.*, 2009, **50**, 127–137.

38 S. L. Li, S. S. Chan, G. Lin, L. Ling, R. Yan, H. S. Chung and Y. K. Tam, *Planta Med.*, 2003, **69**, 445–451.

